Mechanics & Industry **16**, 202 (2015)

DOI: 10.1051/meca/2014075
www.mechanics-industry.org

Mechanics & Industry

Few problems with regularized Coulomb law

Jean-Louis Ligier[a] and Philippe Bonhôte

HEIG-VD, Comatec, 1 route de Cheseaux, 1400 Yverdon-les-bains, Suisse

Received 8 May 2014, Accepted 22 September 2014

Abstract – The main idea is to present some problems where the friction obeys to regularized Coulomb law. Mathematically, it is usual that the friction law is supposed to be the Coulomb law which is controlled by a function "sign" with discontinuity at the origin. In reality, friction phenomenon corresponds to an average continuous behavior. From a modelling point of view, the simplest way to get this continuity is to regularize friction law. Obviously, friction problems become more complicated due to the fact that the friction law exhibits two phases of behavior. Solving problems with this friction law could bring some special results. To present them, the problems considered in this paper are related to the bending of two beams in contact under a certain pressure and to the transversal strain of an elastic thin strip in contact with a rigid body. For these two problems, analytical solutions are presented and also some finite element simulations for comparison.

Key words: Friction / contact / Coulomb / microslip

1 Introduction

Already, Leonardo da Vinci [1] engineers and physicists consider friction in mechanic problems. Particularly in dry friction, it is usual to consider the Coulomb friction. This law of friction is very useful for many problems due to its simplicity. However, it is more and more frequent that the accurate behavior simulation of mechanical systems operating with friction needs to consider refined laws of friction. These laws allow having a better behavior description of the body interfaces in contact. From a practical point of view, the friction law is dependent to the type of problem. For example for metal forming, rubber friction or earthquake, engineers use very different types of law for simulation [2]. It has been observed for instance that in dynamic situation, the interface controls the damping and the stiffness of the joint but these characteristics affect the dynamic response of the complex structures having joints. It could concern the determination of the natural frequencies, the stick-slip phenomenon and the exact location of the components during "stop and go" displacements [3,4] or the impact description of the collision inside a multibody system [5]. In term of quasi static situation, the interface behavior will define the microslip between the different components. This displacement will be important to estimate the fretting risk for example with Ruiz criterion [6], the cumulative microslip between the components of the assembly structure [7,8] or the global stiffness of a conrod with a fitted bearing. Also various situations are considered like dynamic or quasi-static situation, lubricated or dry contact, micro-scale or macro-scale. In this paper, we will focus our analysis on dry friction in quasi static condition at a micro-scale. Quasi-static situation means sliding speed will be lower than few μm.s^{-1}. For this situation, two regimes can be distinguished: pre-sliding regime and gross-sliding regime. For the last one, it corresponds to macro-slip. But pre-sliding regime represents the elastic deformation and the local micro-sliding also called microslip that will occur in the contact interface before macro-slip can be observed. The level of microslip has a strong influence on the contact stiffness in apparently static interfaces. Taking into account this phenomenon from a realistic way will affect the behavior of assembly components or screw joints.

It is well known that the standard Coulomb law does not allow representing this phenomenon. The standard relationship describing the tangential load during sliding at a constant speed v, is:

$$F_{\mathrm{T}} = \mu_0 F_{\mathrm{N}} \mathrm{sign}(v) \tag{1}$$

where μ_0 is the dynamic friction coefficient.

One of the weaknesses of the Coulomb modeling is induced by the fact that the relationship between sliding displacement and the tangential load is discontinue. To

[a] Corresponding author:
Jean-louis.ligier@heig-vd.ch

Nomenclature

a_i	Constants
b	Width beam (mm)
E	Young modulus (MPa)
F_{N}	Normal load (N)
F_{T}	Tangential load (N)
F_{thre}	Threshold load (N)
G	Shear modulus (MPa)
h	Half beam height and plate thickness (mm)
I	Quadratic moment of the cross section (mm^4)
k_i	Constants
K	Stiffness ($\mathrm{MPa}.\mu\mathrm{m}^{-1}$)
K_{T}	Tangential contact stiffness ($\mathrm{MPa}.\mu\mathrm{m}^{-1}$)
k_i	Coefficients
L	Length of the beam or the plate (mm)
M_{f}	Bending moment (Nm)
N	Normal force (N)
P	Pressure (MPa)
P_{r}	Contact pressure (MPa)
S	Normal cross section of the plate (mm^2)
t_{p}	Plate thickness (mm)
T	Shear force (N)
u	Displacement (mm)
U_{N}	Normal displacement due to normal load (mm)
U_{M}	Normal displacement due to bending moment (mm)
v	Velocity ($\mathrm{mm.s}^{-1}$)
w	Bending deflection (mm)
x	Space variable (mm)
X	Location of friction regime change (mm)
y	Space variable (mm)
α	Coefficient (–)
ν	Poisson ratio (–)
μ	Friction factor (–)
μ_0	Dynamic friction factor (–)
σ_{xy}	Shear stress (MPa)
τ	Shear stress at the interface (MPa)
ξ	Space variable

overcome this difficulty, it is quite usual to regularize the Coulomb friction [9]. One easy way consists to adopt the relationship for the tangential force intensity:

$$F_{\mathrm{T}} = \mu_0 F_{\mathrm{N}} \tanh(\alpha u) \tag{2}$$

with F_{N}, F_{T} = normal, tangential load and u the displacement.

But the regularization is not enough realistic for small pre-sliding. Berthoud, Baumberger, Bureau [10,11] have precisely shown the behavior during the pre-sliding regime. At the beginning of the tangential loading the micro-displacement varies linearly with respect to the loading and is elastic. A creep phenomenon follows this displacement but is related to the sliding velocity. To simplify our modelling we consider assembly components in pre-sliding regime where micro-sliding occurs at very low speed in order to neglect the creep period. The regularized Coulomb law adopted in this paper is described in Figure 1.

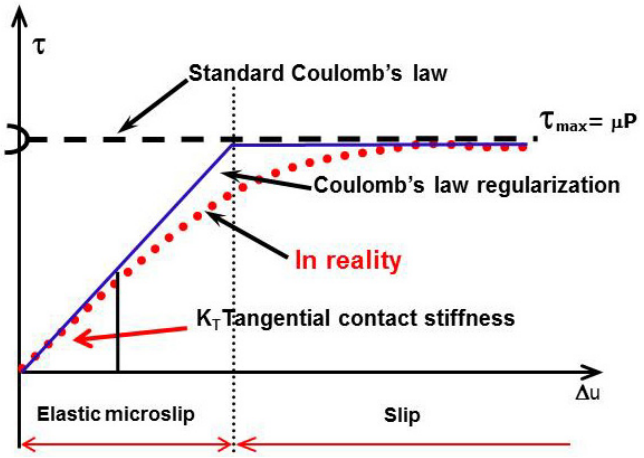

Fig. 1. Coulomb laws.

In the first regime phase, the relation between the shear stress and the displacement is:

$$\tau = K_{\mathrm{T}} \Delta u \tag{3}$$

where Δu corresponds to the relative displacement at the interface between two bodies in contact and K_{T} represents the tangential stiffness.

When the shear stress reaches the Coulomb friction stress, μP, the behavior stops to be elastic.

This behavior is also related to the Iwan model [12] which corresponds to "Coulomb" slider connected to a spring. It is also similar to bristle model used to model dynamic friction [13].

The difficult point with the regularized friction law is to determine the tangential stiffness. It has been shown that the tangential stiffness is due to the elastic response of the interface zone [14] and more particularly to the surface asperities. From the modelling done by Greenwood and Williamson [15], which describes, from a statistical point of view, the normal contact stiffness between rough surfaces, Sherif and Kossa [16] have shown that from a theoretical point of view the tangential stiffness is:

$$K_{\mathrm{T}} = \frac{\pi(1-\nu)}{2(2-\nu)} K_{\mathrm{N}} \tag{4}$$

They have also demonstrated the number of contacts at the interface is proportional to the normal load, the mean size of the elementary contact aera is independent of the normal load, and for relatively low normal load each asperity behaves independently. From an experimental and numerical point of view Gonzalez-Valadez and Medina [17–19] have obtained that the ratio between the two stiffnesses is comprised between 0.5 to 0.7.

From a practical point of view, the normal stiffness could be determined with the Greenwood-Williamson model and the physical and geometrical characteristics could be deduced from the roughness measurements and the relationships proposed by Robbe-Valloire [20]. In microslip regime, the equivalent behavior of the interface is summarized in Figure 2.

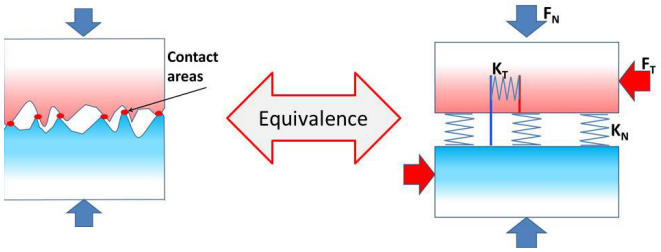

Fig. 2. Stiffness equivalence.

Several devices have been developed to precisely measure precisely the tangential stiffness. With a device using microwaves Valadez and Dwyer-Joyce [17] have confirmed experimentally that for very low load the shear stiffness is directly related to the normal pressure as presented by Berthoud [10].

In this paper we propose the analytical solutions to two problems with regularized friction law. It is quite usual to find solution with standard Coulomb friction but less with regularized Coulomb law. It is also important to highlight that many numerical simulations codes (finite element, multi-body dynamic...) use regularized friction laws. But codes do generally not request the value of the tangential stiffness. Implicitly, the codes use a default value of the stiffness which is very high and proportional to the length of the element. Sometimes the stiffness is inversely proportional to the depth of the element in contact.

As the tangential stiffness is very important in the assembly complex structures, the analytical solutions, determined in this paper, will allow:

- to be able to identify the tangential stiffness with simple experiment measurements;
- to characterize the difference we can get between theory and finite element calculation.

2 Friction problems

As relative displacements at the interface between bodies in contact could result:

- from direct longitudinal effect;
- from indirect transversal effect induced by striction,

two problems with these two effects are solved in this paper. The Coulomb law and regularized are considered. The characteristics of these law are given in Figure 1.

2.1 Twin beams under mutual friction

At first we are looking at a twin cantilever beam system. The cantilever beams are pressed together with a uniform and moderate pressure P. The transverse load applied at the end of the two beams produces friction at the interface as soon as relative displacement appears between the two beams (cf. Fig. 3).

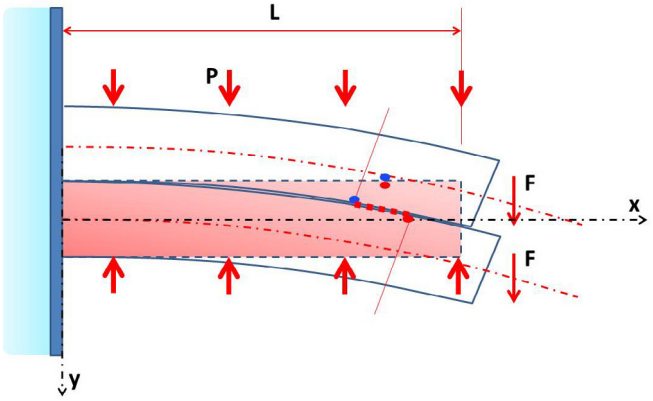

Fig. 3. Twin beams under bending.

The cross section of each beam is rectangular ($b.2h$) with $2h$ for the height of the beam. h is supposed to be quite small in order to neglect shear strain in the beam. Due to the low value of P, transversal and longitudinal strains are negligible and do not introduce behaviour difference between twin beams.

2.1.1 Standard Coulomb friction

Before considering the regularized Coulomb friction the problem is solved with standard Coulomb friction. This kind of friction will occur at the interface between the two beams when the shear stress will be higher than adherence stress between the two beams due to the pressure P. By the way, for low load the two beams remain solidary. They form a beam $4h$ height under a shearing force $2F$. With strength of material [21] we know that the shear stress induced by a shear force $2F$ on a rectangular cross section is:

$$\sigma_{xy}(y) = \frac{3F}{4hb}\left(1 - \left(\frac{y}{2h}\right)^2\right) \tag{5}$$

for y measured from the beam interface.

The deflection is:

$$w(x) = \frac{F}{16Ebh^3}\left(3Lx^2 - x^3\right) \tag{6}$$

Slip at the interface will not occur as shear stress (5) will remain lower than the adherence μP. So, it involves that the loading will be lower than the threshold force F_{thre}:

$$F < F_{\text{thre}} = \frac{4\mu bhP}{3} \tag{7}$$

We consider that the static friction coefficient, μ, is the same than the dynamic friction coefficient to avoid considering a sudden instability when the adherence ceases to maintain the beams solidary. For comparison with finite element, it will be easier.

In the case where slip occurs, the beam deflections will be the same for the two beams and will be due to a new

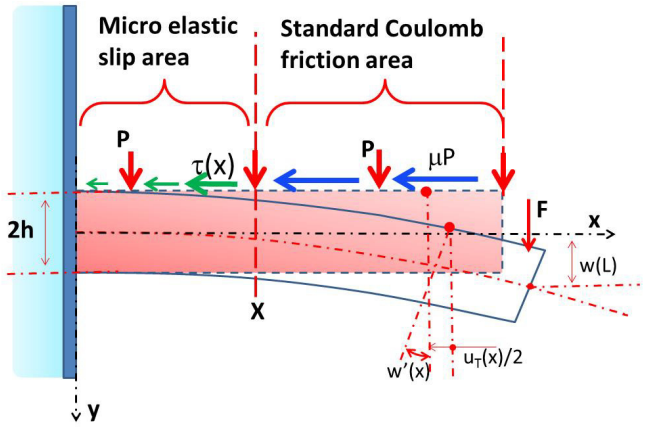

Fig. 4. Beam bending.

bending moment, M_{f}, taking into account the shear stress at the interface. Its expression is:

$$M_{\mathrm{f}} = (F - \mu P bh)(L - x) \tag{8}$$

The deflection, after solving the differential equation of the bending beam, for one beam, will be:

$$w(x) = \frac{(F - \mu P bh)}{4Ebh^3}\left(3Lx^2 - x^3\right) \tag{9}$$

In summary for Coulomb friction, the deflection at the end of the beam will be:

$$\begin{cases} F < F_{\mathrm{thres}} = \dfrac{4\mu bhP}{3}; & w(L) = \dfrac{FL^3}{8Ebh^3} \\ F > F_{\mathrm{thres}} = \dfrac{4\mu bhP}{3}; & w(L) = \dfrac{(F - \mu bhP)L^3}{2Ebh^3} \end{cases} \tag{10}$$

2.1.2 Regularized friction

With regularized law of friction it is necessary to suppose that a part of the interface is subject to micro-elastic-slip and the other one is subject to macro slip as described in Figure 4.

In Figure 4, the new quantity to determine is the shear stress in the micro-elastic-slip area. To do that we must determine the torsor in any cross section of the beam. As the system is symmetric to respect to the interface, we will just analyze the lower beam. So, we have to consider: the normal force, the shearing force and the bending moment which act at the point x along the center line of the lower beam:

$$\text{for } x < X \begin{cases} N(x) = (X - L)\mu bP - b\int_x^X \tau(\xi)\,\mathrm{d}\xi \\ T(x) = F \\ M_f(x) = F(L - x) - (L - X)\mu bhP \\ \qquad\qquad -bh\int_x^X \tau(\xi)\,\mathrm{d}\xi \end{cases} \tag{11}$$

and

$$\text{for } x > X \begin{cases} N(x) = -b\int_x^L \tau(\xi)\,\mathrm{d}\xi \\ T(x) = F \\ M_f(x) = F(L - x) - bh\int_x^L \tau(\xi)\,\mathrm{d}\xi \end{cases} \tag{12}$$

To start the resolution, we must determine the shear stress in the first part of the beam where the shear stress is controlled by micro-elastic-slip regime, it means:

$$\tau(x) = 2K_T\left(u_N(x) + u_M(x)\right) \tag{13}$$

where u_{N} and u_{M} are the displacements of the lower beam due to the normal force and to the bending moment.

The factor 2 takes into account the fact that the upper beam has the same but opposite displacements than the lower beam. The equations which allow determining these displacements are:

$$u_N(x) = \frac{1}{2Eh}\int_0^x \left((X - L)\mu P - \int_x^X \tau(\xi)\,\mathrm{d}\xi\right)\mathrm{d}x \tag{14}$$

$$u_M(x) = hw'(x) \tag{15}$$

and

$$w''(x) = \frac{3}{2Ebh^3}\Big(F(L - x) - (L - X)\mu bhP - bh\int_x^X \tau(\xi)\,\mathrm{d}\xi\Big) \tag{16}$$

After deriving the shear stress equation and combining with the four previous equations, the relationship defining the shear stress is:

$$\tau''(x) - k_0^2\tau(x) = -k_1 F \tag{17}$$

with

$$k_0 = 2\sqrt{\frac{K_T}{Eh}}, \quad k_1 = \frac{3K_T}{Ebh^2}$$

Taking into account that the shear stress is null for $x = 0$ and is equal to the Coulomb shear stress for $x = X$, the solution of the differential equation is:

$$\tau(x) = \frac{k_1}{k_0^2}F(1 - \cosh(k_0 x)) + \left(\mu P k_0^2 + k_1 F(\cosh(k_0 X) - 1)\right)\frac{\sinh(k_0 x)}{k_0^2\sinh(k_0 X)} \tag{18}$$

With this new expression of the interface shear stress, it is now possible to solve the bending equation in order to obtain the bending deflection. After solving the equation and considering the boundary condition of the cantilever beam, the deflection solution is:

$$w(x) = k_5\frac{x^2}{2} + k_2 F\frac{x^3}{6} + k_6(\cosh(k_0 x) - 1) + k_7(\sinh(k_0 x) - k_0 x) \tag{19}$$

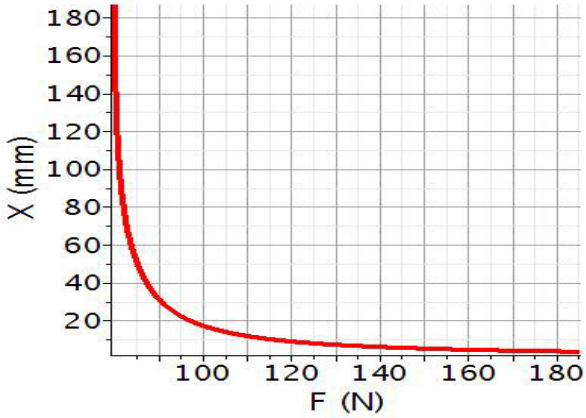

Fig. 5. X variations with respect to F.

where

$$k_2 = \frac{-3}{8Ebh^3}, \quad k_4 = \frac{-9F}{8Ebh^3}, \quad k_6 = \frac{k_3}{k_0^3}, \quad k_7 = \frac{k_4}{k_0^3},$$
$$k_3 = \frac{3}{8hK_T \sinh(k_0 X)} \left(\mu P k_0^2 + k_1 F \left(\cosh(k_0 X) - 1\right)\right),$$
$$k_4 = \frac{-9F}{8Ebh^3}, \quad k_6 = \frac{k_3}{k_0^3}, \quad k_7 = \frac{k_4}{k_0^3},$$
$$k_5 = -k_2 F X - \cosh(k_0 X)\frac{k_3}{k_0} - \sinh(k_0 X)\frac{k_4}{k_0} + \frac{3\left(L - X\right)}{2Ebh^3}\left(F - \mu h b P\right)$$

The expression of the bending deflection can be introduced in the shear stress equation. But the shear stress at $x = X$ must be equal to the Coulomb friction. This last condition is used to determine X. So, we obtain the following equation to solve:

$$\tau\left(X\right) = K_T\left(u_N\left(X\right) - u_M\left(X\right)\right) = \frac{\mu P}{K_\mathrm{T}} \tag{20}$$

This equation has not an analytical solution and must be solved numerically. The numerical data we consider are close to those of a test bench. Tangential stiffness is deduced of the beams roughness $R = 3.1$ μm and relationship (19). Numerical date is the following:

$$L = 200 \text{ mm}, E = 210 \text{ GPa}, h = 10 \text{ mm}, b = 20 \text{ mm},$$
$$P = 1 \text{ MPa}, \mu = 0.3, K_\mathrm{T} = \mu P/5e - 4 \text{ MPa.mm}^{-1}$$

After solving numerically the previous equation we get X with respect to F. Figure 5 gives the evolution of X. It can be observed that for certain loadings, X can be higher than the length of the beam. In that case, there is only one regime of friction along the beam interface. This situation will be detailed further away.

As X can be determined, we can write the deflection and the slope at $x = X$:

$$w\left(X\right) = k_5\frac{X^2}{2} + k_2 F\frac{X^3}{6} + k_6\left(\cosh(k_0 X) - 1\right) + k_7\left(\sinh(k_0 X) - k_0 X\right)$$
$$w'\left(X\right) = k_5 X + k_2 F\frac{X^2}{2} + k_6 k_0 \sinh(k_0 X) + k_7 k_0\left(\cosh(k_0 X) - 1\right) \tag{21}$$

These expressions will constitute the boundary conditions for the second part of the beam. In that case, the bending moment is known and the resolution is quite usual and gives for the deflection in $x = L$, called $w_T(L)$:

$$w_\mathrm{T}\left(L\right) = \frac{\left(F - \mu P b h\right)}{12Ebh^3}\left(L - X\right)^3 + w'\left(X\right)\left(L - X\right) + w(X) \tag{22}$$

Equation (22) represents the deflection solution for the case where the two regimes of friction exist along the interface.

For the situation where the only friction regime is micro-elastic-slip ($X > L$), the loading torsor is quite simple:

$$\begin{cases} N\left(x\right) = -b\int_x^L \tau\left(\xi\right)\mathrm{d}\xi \\ T\left(x\right) = F \\ M_f\left(x\right) = F\left(L - x\right) - bh\int_x^L \tau\left(\xi\right)\mathrm{d}\xi \end{cases} \tag{23}$$

The resolution is similar to the previous one. The differential equation determining the shear stress is the same. However, there is a new boundary condition:

$$\text{for } x = L, \quad \tau\left(L\right) = K_T u_T\left(L\right) \tag{24}$$

Then, the solution for the shear stress becomes:

$$\tau\left(x\right) = \frac{k_1}{k_0^2}F\left(1 - \cosh(k_0 x)\right) + \left(u_T\left(L\right)k_0^2 K_T + k_1 F\left(\cosh(k_0 L) - 1\right)\right)\frac{\sinh(k_0 x)}{k_0^2 \sinh(k_0 L)} \tag{25}$$

The calculation of the beam deflection gives the solution

$$w\left(x\right) = k_8\frac{x^2}{2} + k_2 F\frac{x^3}{6} + k_{10}\left(\cosh(k_0 x) - 1\right) + k_7\left(\sinh(k_0 x) - k_0 x\right) \tag{26}$$

where

$$k_8 = -k_2 F L - \cosh(k_0 L)\frac{k_9}{k_0} - \sinh(k_0 L)\frac{k_4}{k_0}, k_{10} = \frac{k_9}{k_0^3}$$
$$k_9 = \frac{3}{8hK_T \sinh(k_0 L)}\left(u_T\left(L\right)K_T k_0^2 + k_1 F\left(\cosh(k_0 L) - 1\right)\right)$$

The solution of the beam deflection is expressed with respect to the total displacement $u_T(L)$. It involves calculating this term. So, we have to define u_N and u_M for this new situation.

For the displacement induced by the normal force, the relationship is:

$$u_N(L) = \frac{1}{2Eh}\int_0^L \left(-\int_x^L \tau(\xi)\,d\xi\right) dx \tag{27}$$

After calculation, we get:

$$u_N(L) = k_{11}F + k_{12}u_T(L) \tag{28}$$

with

$$k_{11} = \frac{k_1 L}{4Ehk_0^3}\left(k_0 L - \tanh\left(\frac{k_0 L}{2}\right)\right),$$
$$k_{12} = \frac{K_T}{2Ehk_0^2}\left(k_0 L \coth(k_0 L) - 1\right)$$

For the displacement induced by the bending we have:

$$u_M(L) = hw'(L) \tag{29}$$

After calculation and using previous results, we obtain:

$$u_M(L) = k_{13}F + k_{14}u_T(L) \tag{30}$$

with

$$k_{13} = k_2 h\frac{L^2}{2} + \frac{3hk_1 L}{2\sinh(k_0 L)\,Ehk_0^3}\left(1 - \cosh(k_0 L)\right),$$
$$k_{14} = \frac{3K_T}{2Ehk_0^2}\left(k_0 L \coth(k_0 L) - 1\right)$$

As

$$u_T(L) = 2\left(u_N(L) + u_M(L)\right) \tag{31}$$

we can get the relationship:

$$u_T(L) = \frac{-2\left((k_{11} + k_{13})\right)F}{\left(1 + 2\left(k_{12} + k_{14}\right)\right)} \tag{32}$$

For this situation, the bending deflection at the end of the beam is proportional to F.

$$w(L) = k_8\frac{L^2}{2} + k_2 F\frac{L^3}{6} + k_{10}\left(\cosh(k_0 L) - 1\right) + k_7\left(\sinh(k_0 L) - k_0 L\right) \tag{33}$$

2.1.3 Numerical simulation and comparison

It is interesting to plot the deflection with respect to F for different values of K_T. It allows assessing the K_T influence, particularly with respect to the standard Coulomb friction. It also shows the possibility to assess the micro-contact elasticity by measuring the deflection at the end of the beam. With the same numerical data than previously, we can obtain the following plots for various K_T (cf. Fig. 6). In Figure 6, it can be observed that the difference between the two approaches, standard Coulomb friction and regularized Coulomb friction, is not so important. As it is quite easy to modify the tangential stiffness by modifying the roughness, we simulate the case where the nominal tangential stiffness is divided by 5. Results are plotted in Figure 7. In that case, we can observe a strong difference which could be easy to detect by measurements. These differences highlight the importance to correctly choose K_T.

For the comparison with finite element method, we have simulated the problem with Ansys. The mesh used for the simulation is illustrated in Figure 8. 2000 quadratic plane stress elements have been used for the mesh and quadratic contact elements surface to surface model the

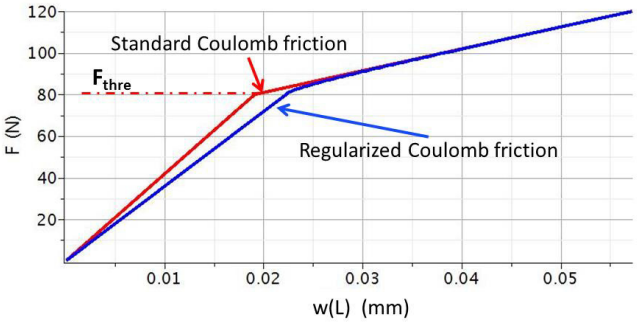

Fig. 6. Deflection for the two friction laws.

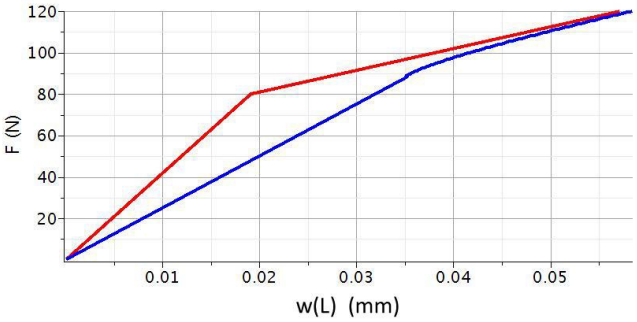

Fig. 7. Reduced tangential stiffness.

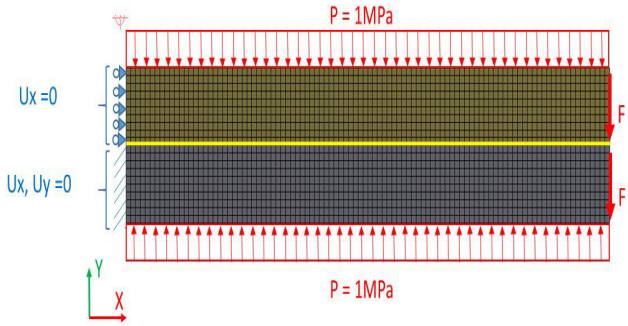

Fig. 8. Finite element model.

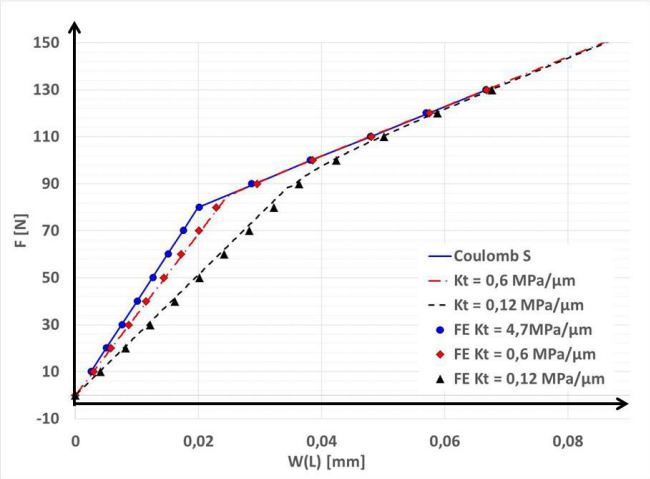

Fig. 9. Comparison analytical and F.E. solutions.

interface. More refined meshes have also been tested but no numerical modifications of the results have been observed. The important point to notice is that finite element codes use a certain value of K_{T} by default. However, this K_{T} value depends to the mesh size. It involves that for accurate slip values at the interface, the tangential stiffness has to be imposed by the user. Several resolution methods have also been tested (penalty, Lagrange, augmented Lagrange) and each one gives the same results.

Implicitly, with the friction orientation, monotonic loading is supposed. After performing various finite element calculations, we get the comparison between analytical solution and numerical solution. In Figure 9, we can observe that analytical and numerical solutions are very close.

In summary, this modelling shows:

- a very good agreement between finite element and analytical approach. Thus, analytical approach can be used as benchmark for new contact element. It could help to evaluate error introduced by the use of shell element in this kind of problem. It can also determine:
- when simplifying assumption of the analytical model is not valid. For instance, when the beam thickness possesses non negligible shear strain;
- the importance to control K_{T}, usually given by default in finite element code;
- an experimental way to identify K_{T} and μ by deflection measurements. Curve slope variation (cf. Fig. 11) is directly related to μ and the change location will determine K_{T}.

2.2 Plate friction

For the second problem, we consider a situation where we can get an analytical solution to compare with finite elements results. For this case the longitudinal displacement is due to striction effect induced by the contact

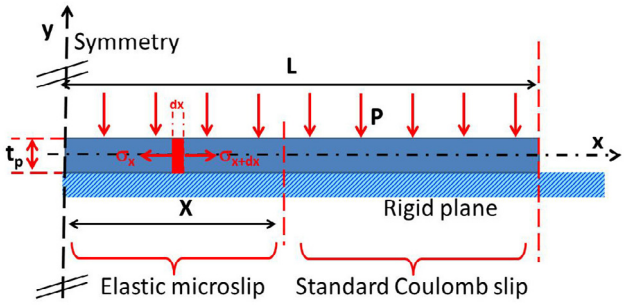

Fig. 10. Plate on the rigid plane.

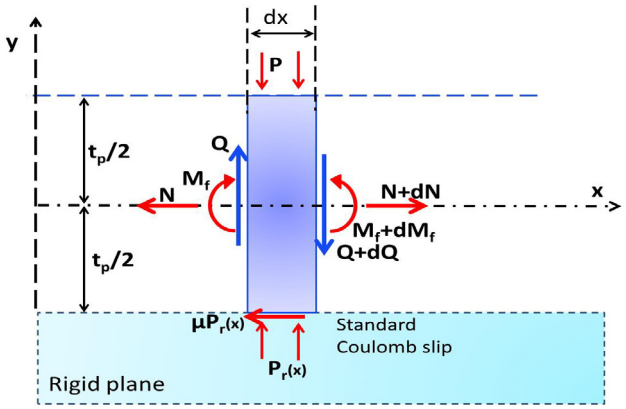

Fig. 11. Equilibrium of an elementary strip.

pressure. Let a plate lying on a rigid plan. The friction between the plate and the rigid surface obeys to a regularized Coulomb law as described in Figure 10. The plate is supposed to be quite wide as we can consider the problem in strain plane situation (width $\gg$ length). As the thickness of the plate, t_{p}, is sufficiently thin, we can neglect shear strain in the plate. A pressure P is applied on the upper surface of the plate as illustrated in Figure 10.

2.2.1 Contact pressure

Before solving the problem it is interesting to show that contact pressure between the beam and the rigid plane is mainly constant and equal to P, to do that we must consider an elementary strip of beam as described in Figure 11.

The strip equilibrium brings the equations:

$$\begin{cases} \dfrac{\mathrm{d}Q}{\mathrm{d}x} = P_r\left(x\right) - P \\ \dfrac{\mathrm{d}M_f}{\mathrm{d}x} = Q + \mu h P_r\left(x\right) \end{cases} \tag{34}$$

with M_{f} = bending moment and Q = shear load.

As the plate remains straight in its contact with the rigid plane, it involves that the second and the third derivation of the deflection, called $y(x)$, are null along the

x axis. Mathematically, it is expressed by the relationship:

$$y'''(x) = \frac{M_f'}{EI} - \frac{k}{GS}Q'' \tag{35}$$

with EI = flexural rigidity modulus, GS = shear rigidity modulus, k = shear correction factor.

Reintroducing equilibrium equations (34) in this deflection equation (35) gives:

$$\frac{GS}{kEI}\left(Q + \mu h Q' + \frac{\mu t_p}{2}P\right) - Q'' = 0 \tag{36}$$

The general solution is:

$$Q = -\frac{\mu t_p}{2}P + \mathrm{e}^{ax}\left(A\cosh(a_2 x) + B\sinh(a_2 x)\right) \tag{37}$$

with

$$a_1 = \frac{\mu t_p GS}{kEI}; \quad a_2 = \sqrt{\left(\frac{2a_1}{\mu t_p}\right)^2 + 2a_1}$$

Taking into account the boundary condition $Q(0) = 0$ and $Q(L) = 0$, the previous expression becomes:

$$Q = \frac{\mu t_p}{2}P\left[\mathrm{e}^{a_1 x}\left(\cosh(a_2 x) - B\sinh(a_2 x)\right) - 1\right] \tag{38}$$

with

$$B = \frac{\mathrm{e}^{-a_1 L} - \cosh(a_2 L)}{\sinh(a_2 L)}$$

The contact pressure below the plate, P_r, is easily obtained by

$$P_\mathrm{r} = P + \frac{\mathrm{d}Q}{\mathrm{d}x} \tag{39}$$

With the previous numerical application the pressure field is illustrated in Figure 12.

With this numerical result, we can accept to consider Pr as quasi constant. This hypothesis failed when the ratio L/h becomes lower than 20.

2.2.2 Modelling

For symmetry reasons, the half-length of the plate is represented. To respect the regularized Coulomb law the first part of the plate is subject to elastic microslip and the last one is concerned by Coulomb slip. The equilibrium of an elementary vertical layer in the elastic microslip area provides the relationship:

$$\frac{\mathrm{d}\sigma_x}{\mathrm{d}x} = \frac{K_\mathrm{T}}{t_\mathrm{p}}u(x) \tag{40}$$

where $u(x)$ represents longitudinal displacement at location x.

Using elastic behavior relationships in plane strain and taking into account that the vertical normal stress is equal to $-P$, we get:

$$\frac{\mathrm{d}u(x)}{\mathrm{d}x} = \frac{1}{E}\left(\left(1-\nu^2\right)\sigma_x + \nu(1+\nu)P\right) \tag{41}$$

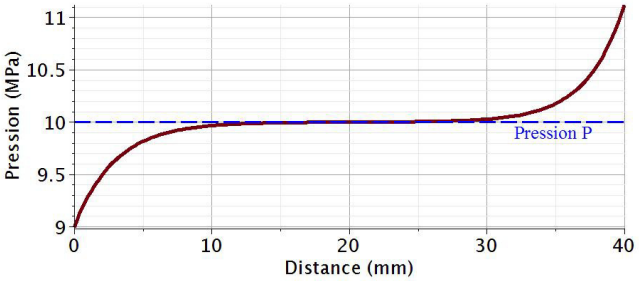

Fig. 12. Pressure field.

Equation (40) becomes:

$$\frac{\mathrm{d}^2u(x)}{\mathrm{d}x^2} = \frac{\left(1-\nu^2\right)K_\mathrm{T}}{t_\mathrm{p}E}u(x) \tag{42}$$

The general solution with symmetry condition and for the area $0 < x < X_r$ is (subscript "r" is used to remind it concerns the regularized Coulomb friction, subscript "s" will be for the standard Coulomb friction).

$$u(x) = A\sinh(\alpha x) \tag{43}$$

with

$$\alpha = \sqrt{\frac{\left(1-\nu^2\right)K_T}{t_\mathrm{p}E}}$$

For the second part of the plate, $x > X_r$, equilibrium condition of a vertical elementary strip, expressed in term of displacement, provides the following differential equation:

$$\frac{\mathrm{d}u(x)}{\mathrm{d}x} = \frac{P}{E}\left(\frac{\left(1-\nu^2\right)\mu(x-L)}{t_\mathrm{p}} + \nu(1+\nu)\right) \tag{44}$$

The solution for the displacement for $x > X_r$, is:

$$u(x) = \frac{P}{E}\left(\begin{array}{l}\frac{\left(1-\nu^2\right)\mu\left(x^2/2 - X_r^2/2 - L(x-X_r)\right)}{t_p} \\ +\nu(1+\nu)(x-X_r)\end{array}\right) + \frac{\mu P}{K_T} \tag{45}$$

At the end of the plate we get:

$$u(L) = \frac{P(L-X_r)}{E}\left(\frac{\left(1-\nu^2\right)\mu(L-X_r)}{2t_p} + \nu(1+\nu)\right) + \frac{\mu P}{K_T} \tag{46}$$

The connection between the two parts of the plate is obtained by considering that for $x = X_r$:

$$u(X_r) = \frac{\mu P}{K_\mathrm{T}} \text{ and } t_p\sigma(X_r) = -\mu P(L - X_r) \tag{47}$$

The first condition of equation (47) involves that:

$$A = \frac{\mu P}{K_T \sinh(\alpha X_r)} \tag{48}$$

The second one becomes a transcendent equation:

$$\frac{t_p E \mu \alpha}{(1-\nu^2) K_T \tanh(\alpha X_r)} = \frac{\nu t_p}{1-\nu} - \mu (L - X_r) \quad (49)$$

It is interesting to notice that the X_r solution is independent to P. Generally, this equation has no analytical solution. But for high value of X_r, we can get an approximated solution by considering that the term $\tanh(\alpha X_r)$ is equivalent to 1. Then the solution becomes:

$$X_r \approx L + \frac{t_p E \alpha}{(1-\nu^2) K_T} - \frac{\nu t_p}{\mu (1-\nu)} \quad (50)$$

To complete this approach, the solution for standard Coulomb friction law is considered. After solving the differential equation (44), the general displacement solution is:

$$u(x) = \frac{P}{E}\left((1-\nu^2)\frac{\mu}{t_p}\left(\frac{x^2}{2} - Lx\right) + \nu(1+\nu)x\right) + \text{cste} \quad (51)$$

The integration constant will be defined by the condition:

$$u(X_s) = 0$$

Then, the transition between stick zone and slip zone, defined by X_s, verifies the condition that the axial strain is null and axial strain is obtained by deriving equation (51):

$$X_s = \left(L - \frac{\nu t_p}{(1-\nu)\mu}\right) \quad (52)$$

It follows that the displacement at the end of the plate will be:

$$u(L) = \frac{(1+\nu)\nu^2 t_p P}{(1-\nu)\mu E} \quad (53)$$

2.2.3 Numerical simulation and comparison

In finite element simulation we cannot treat the problem by using beam or shell element in which no striction effect under transversal pressure is considered. Plane strain elements are used. The mesh is represented in Figure 13. Refined meshes have also been tested and no difference has been noted.

At this stage we can perform some comparisons between the different approaches. The numerical application we consider is:

$$L = 10 \text{ mm}, t_P = 0.2 \text{ mm}, E = 70 \text{ GPa}, \nu = 0.3,$$
$$\mu = 0.3, P = 10 \text{ MPa}.$$

In Figure 14, the displacement at the end of the plate, $u(L)$, shows big variation for low K_T values. Such variations may be due to large variations in roughness.

In order to detect some difference between analytical and finite element solution we can look at the X value with respect to the friction coefficient and the tangential stiffness (cf. Fig. 15). This parameter must vary between 0 and L.

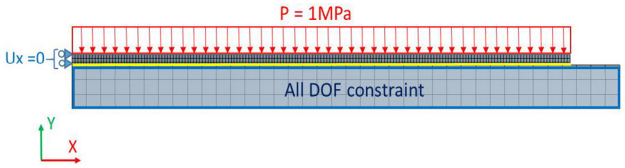

Fig. 13. Plate mesh.

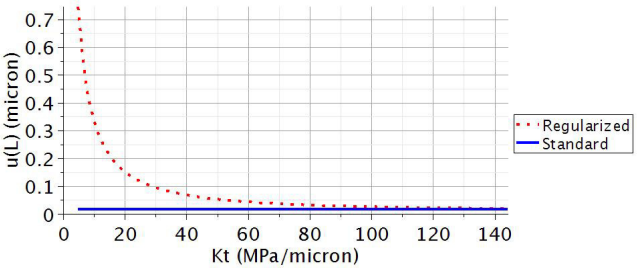

Fig. 14. Displacement comparison.

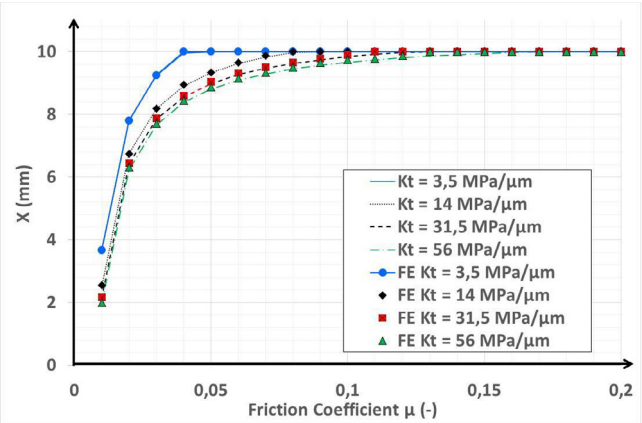

Fig. 15. X with respect to friction and stiffness.

In summary of this squeezed plate problem, it is found:

- a contact pressure model which allows to determine if contact pressure can be considered as constant;
- very good agreement between finite element and analytical solutions. As mentioned earlier, the analytical approach can be used as benchmark for new contact element. It could help to evaluate error introduced by the use of shell element in this kind of problem. It can also determine when simplifying assumption of the analytical model is not valid;
- a perfect bonding occurs for high friction coefficient;
- roughness and pressure contact control the location of slipping interface.

3 Conclusion

The consideration of the regularized Coulomb friction in the behavior of assembly complex structures allows to get more realistic response particularly in the microslip regime. During a loading, it involves a better prediction of slipping area instead a sudden slip of the whole interface with the standard Coulomb law.

The cantilever twin beams problem has shown possibilities to assess tangential stiffness and friction coefficient by beam deflection measurements. It has also been shown that simulation with finite element code needs to be accurate on the implicit tangential stiffness used in code to get realistic results like relative displacements between two bodies in contact.

The problem of a plate squeezed on a rigid plan provides an analytical solution which allows assessing some behavior differences between regularized and standard Coulomb friction law and between analytical solution and finite element simulation.

By default, finite element codes try to get Coulomb friction but mesh size modifies the K_T default value.

The two analytical solutions obtained in this paper can be used as benchmark solutions.

References

[1] D. Dowson, History of tribology. 2nd edn., John Wiley, 1998

[2] V.L. Popov, Contact mechanics and friction, physical principles and application, Springer Verlag, 2010

[3] Y. Song et al., Simulation of dynamics of beam structures with bolted joints using adjusted Iwan beam elements, J. Sound. Vib. 273 (2004) 249–276

[4] H.A. Sherif, Effect of contact stiffness on the establishment of self-excited vibrations, Wear 141 (1991) 227–234

[5] P. Flores, J. Ambrosio, J.C.P. Claro, H.M. Lankarani, Influence of the contact-impact model on the dynamic response of multi-body systems, ImechE 2006, Vol. 220, Part K, pp. 21–34.

[6] K. Anandavel, R.V. Prakash, Extension of Ruiz criterion for evaluation of 3-D fretting fatigue damage parameter, Procedia Engineering 55 (2013) 655–660

[7] J.-L. Ligier, N. Antoni, Cumulative microslip in conrod big end bearing system, ASME 8-10 (2006)

[8] N. Antoni, Q.-S. Nguyen, J.-L. Ligier, P. Saffré, J. Pastor, On the cumulative microslip phenomenon, Eur. J. Mech. – A/Solids 26 (2007) 626–646

[9] D.D. Quinn, A new regularization of Coulomb friction, J. Vib. Acoust. 126 (2004) 391–397

[10] P. Berthoud, T. Baumberger, Shear stiffness of a solid–solid multicontact interface, Proc. R. Soc. Lond. A 454 (1998) 1615–1634

[11] L. Bureau, T. Baumberger, C. Caroli, O. Ronsin, Low velocity friction between macroscopic solids. C. R. Acad. Sci. Paris, t.2, Serie IV, 2001, pp. 699–707

[12] W.D. Iwan, A distributed element model for hysteresis and its steady–state dynamic response, ASME J. Appl. Mech. 33 (1966) 893–900

[13] J. Liang, S. Fillmore, O. Ma, An extended bristle friction force model with experimental validation, Mech. Mach. Theory 56 (2012) 91–100

[14] J.J. O'Connor, K.L. Johnson, The role of surface asperities in transmitting tangential forces between metals, Wear 6 (1963) 118–139

[15] J.A. Greenwood, J.B.P. Williamson, Contact of nominally flat surfaces, Proc. R. Soc. Lond. A 295 (1966) 300

[16] H.A. Sherif, S.S. Kossa, Relationship between normal and tangential contact stiffness of nominally flat surfaces, Wear 151 (1991) 49–62

[17] M. Gonzalez-Valadez, A. Baltazar, R.S. Dwyer-Joyce, Study of interfacial stiffness ratio of a rough surface in contact using a spring model, Wear 268 (2010) 373–379

[18] M. Gonzalez-Valadez, R.S. Dwyer-Joyce, On the interface stiffness in rough contacts using ultrasonic waves, Ingenieria Mecanica 3 (2008) 29–36

[19] S. Medina, D. Nowell, D. Dini, Analytical and numerical models for tangential stiffness of rough elastic contacts, Tribol. Lett. 49 (2013) 103–115

[20] F. Robbe-Valloire, Statistical analysis of asperities on a rough surface, Wear 249 (2001) 401–408

[21] S. Timoshenko, Résistance des matériaux, Dunod, 1990